Journal of Marine Science and Technology

Volume 23 | Issue 2 Article 8

VOLTAGE SAG PLANNING OF A POWER SYSTEM WITH SPECIALLY CONNECTED TRANSFORMERS USING HYBRID DIFFERENTIAL EVOLUTION CONSIDERING ITI CURVE

Yao-Hung Chan
Department of Electrical Engineering, National Taiwan University of Science and Technology, Taipei 106, Taiwan, R.O.C., cyp@nkut.edu.tw

Chi-Jui Wu
Department of Electrical Engineering, National Taiwan University of Science and Technology, Taipei 106, Taiwan, R.O.C.

Ying-Pin Chang
Department of Electrical and Information Engineering, Nan Kai University of Technology, Nantou, Taiwan, R.O.C.

Recommended Citation

Chan, Yao-Hung; Wu, Chi-Jui; and Chang, Ying-Pin (2015) "VOLTAGE SAG PLANNING OF A POWER SYSTEM WITH SPECIALLY CONNECTED TRANSFORMERS USING HYBRID DIFFERENTIAL EVOLUTION CONSIDERING ITI CURVE," *Journal of Marine Science and Technology*: Vol. 23: Iss. 2, Article 8.
DOI: 10.6119/JMST-014-0515-2
Available at: https://jmstt.ntou.edu.tw/journal/vol23/iss2/8

Journal of Marine Science and Technology, Vol. 23, No. 2, pp. 202-211 (2015)
DOI: 10.6119/JMST-014-0515-2

VOLTAGE SAG PLANNING OF A POWER SYSTEM WITH SPECIALLY CONNECTED TRANSFORMERS USING HYBRID DIFFERENTIAL EVOLUTION CONSIDERING ITI CURVE

Yao-Hung Chan[1], Chi-Jui Wu[1], and Ying-Pin Chang[2]

Key words: voltage sag, power quality, ITI curve, hybrid differential evolution method, specially connected transformers.

ABSTRACT

This paper outlines the voltage sag planning of a power system with a three-phase to two-phase transformer. We compared systems with V-V and Scott connection schemes using the hybrid differential evolution (HDE) method to determine the design parameters by taking into account the ITI curves and coordination of over-current relays. The proposed model comprises a node admittance matrix for the calculation of voltage sag in order to determine the severity of system sag after single or two-phase faults. These analytical equations are useful in the mathematical determination of optimal design parameters. We also used the proposed method to obtain suitable values for the relay time multiplier and transformer impedance. Experiment results on V-V and Scott power systems demonstrate that the severity of voltage sag can be reduced through the tuning of relay settings and transformer impedance.

I. INTRODUCTION

Voltage sag is an index of power quality degradation, which is useful in the study of fault events. A number of momentary faults can cause voltage sag in the period prior to the activation of protective relays. One previous study on voltage sag revealed that system voltage can be reduced to between 10% and 90% of its normal value within just a few cycles (IEEE Standard 446, 1995; IEEE Standard 1159, 1995; Bollen 1999; IEEE Standard 1100, 2005). This study investigated this issue from three perspectives: drop in the voltage (ΔV) (Das 1990; Mahdianpoor et al., 2011), duration (Δt) (Yalcinkaya et al., 1998), and the possible number (Wang et al., 2005). ΔV is determined by system impedances and type of fault whereas Δt is determined by the nature of the protective relays and the circuit breakers. Fig. 1 indicates the severity of voltage sag; i.e., $\Delta V \times \Delta t$. Limits related to the severity of voltage sag are defined for consumer electronic products, large electrical equipment, and semiconductor manufacturing machines. Fig. 2 presents one such limit designated by the Information Technology Industry Council (ITIC) (Heydt and Jewell, 1998; Heydt et al.,

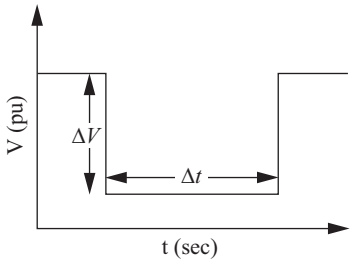

Fig. 1. Voltage sag characteristics.

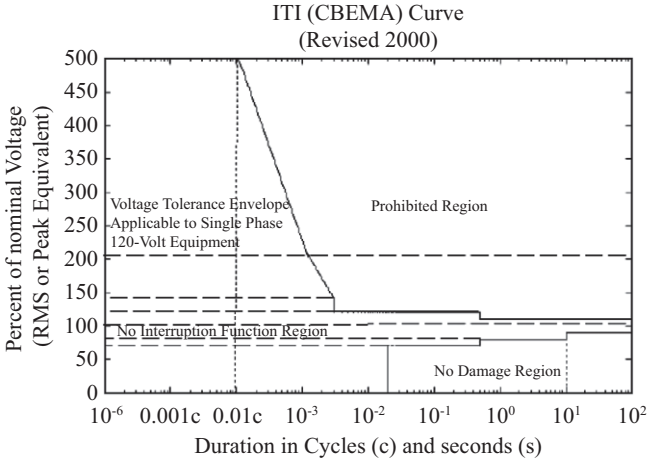

Fig. 2. ITI power acceptability curve.

Paper submitted 12/26/12; revised 05/15/14; accepted 05/15/14. Author for correspondence: Ying-Pin Chang (e-mail: cyp@nkut.edu.tw).

[1] *Department of Electrical Engineering, National Taiwan University of Science and Technology, Taipei 106, Taiwan, R.O.C.*

[2] *Department of Electrical and Information Engineering, Nan Kai University of Technology, Nantou, Taiwan, R.O.C.*

2001; Gomez and Morcos, 2002a; Gomez and Morcos, 2002b; Kyei et al., 2002; Lee et al., 2004). Semiconductor Equipment and Materials International (SEMI) has also developed the SEMI curve to define the ability of semiconductor devices and equipment to withstand the effects of voltage sag.

Many electrical systems require strong single-phase power sources and special connection schemes, such as V-V, Scott, and Le Blanc, are used to reduce disturbances resulting from voltage unbalance in three-phase sources. In particular, these schemes have been employed in railway electrification systems, which must deal with traction loads on three-phase utility systems. Simplified transformer models using special connections have been used in studies on three-phase power flow (Chen, 1994). Chen and Kuo (1995) proposed a network model to investigate the effects of voltage imbalance. Huang et al. (2001) presented the short-circuits and the load characteristics of specially connected transformers (Huang et al., 2006).

Nonetheless, the issue of voltage sag in specially connected transformers has largely been disregarded. Research was required for the development of equivalent models for three-phase power flow in transformers, network models for unbalanced effects, and short-circuits current models for fault analysis.

This paper presents a means of calculating short circuit voltage and currents in power systems with specially connected transformers using a node admittance matrix. The issue of voltage sag planning is solved using the HDE method, which is a parallel search method that involves accelerating and migrant operations to prevent falling into local optimal solutions (Chiou and Wang, 1998; Lin et al., 2000; Chang and Wu, 2005; Hung et al., 2012). This method of optimization makes it possible to determine system parameters for equipment over a wide range. Transformer impedance and time multiplier settings of the protective relay were adopted as variables. The convergent characteristics of this approach were compared with those of a neural network and our calculation results were compared with ITI curves. Our results demonstrate the efficacy of the proposed system in reducing the severity of voltage sag in power systems with the specially connected transformers.

II. EQUIVALENT ADMITTANCE MODELING OF TRANSFORMERS

Analytical models are required for the optimization of three-phase to two-phase specially connected transformers using V-V, Scott, and Le Blanc connection schemes. Models are developed for winding connections and phase coordinates by taking into account copper losses and phase-angle displacement between the primary and secondary voltages. Let $k_1 = \frac{N_1}{N_2}$ and $k_2 = \frac{N_2}{N_1}$ denote the turn ratios of each phase, where y_t represents the equivalent admittance of series impedance for each of the single-phase transformers used in the short circuit tests.

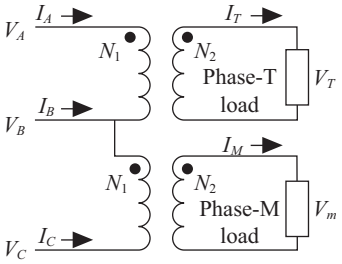

Fig. 3. V-V connection scheme.

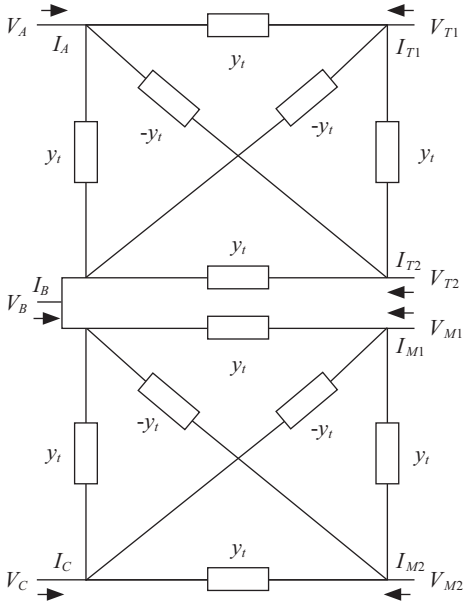

Fig. 4. Equivalent circuit of V-V connection scheme.

1. V-V Connection

As shown in Fig. 3, the V-V connection scheme comprises two single-phase transformers. Three-phase power is used on the primary side to supply two single-phase loads on the secondary side; i.e., the main transformer (M) and the teaser transformer (T). Phasor voltages and currents are presented in (1) and (2), respectively:

$$\begin{bmatrix} V_T \\ V_M \end{bmatrix} = k_2 \begin{bmatrix} 1 & -1 & 0 \\ 0 & 1 & -1 \end{bmatrix} \begin{bmatrix} V_A \\ V_B \\ V_C \end{bmatrix} \tag{1}$$

$$\begin{bmatrix} I_A \\ I_B \\ I_C \end{bmatrix} = k_2 \begin{bmatrix} 1 & 0 \\ -1 & 1 \\ 0 & -1 \end{bmatrix} \begin{bmatrix} I_T \\ I_M \end{bmatrix} \tag{2}$$

As shown in Fig. 4, the equivalent circuit can be made available using the interconnection method. The node-voltage analysis of a three-phase to two-phase transformer can be presented in matrix form, as follows:

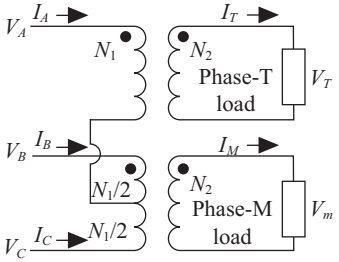

Fig. 5. Scott connection scheme.

$$\begin{bmatrix} I_A \\ I_B \\ I_C \\ I_{T1} \\ I_{T2} \\ I_{M1} \\ I_{M2} \end{bmatrix} = Y \begin{bmatrix} V_A \\ V_B \\ V_C \\ V_{T1} \\ V_{T2} \\ V_{M1} \\ V_{M2} \end{bmatrix} \tag{3}$$

where $I_{T2} = -I_{T1} = I_T$ and $I_{M2} = -I_{M1} = I_M$.

The node admittance matrix (bus admittance matrix) can be expressed as

$$Y = \begin{bmatrix} y_t & -y_t & 0 & -y_t & y_t & 0 & 0 \\ 0 & 2y_t & -y_t & y_t & -y_t & -y_t & y_t \\ 0 & -y_t & y_t & 0 & 0 & y_t & -y_t \\ -y_t & y_t & 0 & y_t & -y_t & 0 & 0 \\ y_t & -y_t & 0 & -y_t & y_t & 0 & 0 \\ 0 & -y_t & y_t & 0 & 0 & y_t & -y_t \\ 0 & y_t & -y_t & 0 & 0 & -y_t & y_t \end{bmatrix} \tag{4}$$

2. Scott Connection

Fig. 5 illustrates the Scott connection scheme, comprising two different turn ratio transformers. The main transform (phase M) has a center-tapped winding on the primary side, and a single winding on the secondary side. The teaser transformer (phase T) is a single-phase transformer. The phase difference between M and T is 90°. Phasor voltage and current are presented in (5) and (6), respectively:

$$\begin{bmatrix} V_T \\ V_M \end{bmatrix} = k_2 \begin{bmatrix} 2/\sqrt{3} & -1/\sqrt{3} & -1/\sqrt{3} \\ 0 & 1 & -1 \end{bmatrix} \begin{bmatrix} V_A \\ V_B \\ V_C \end{bmatrix} \tag{5}$$

$$\begin{bmatrix} I_A \\ I_B \\ I_C \end{bmatrix} = k_2 \begin{bmatrix} 2/\sqrt{3} & 0 \\ -1/\sqrt{3} & 1 \\ -1/\sqrt{3} & -1 \end{bmatrix} \begin{bmatrix} I_T \\ I_M \end{bmatrix} \tag{6}$$

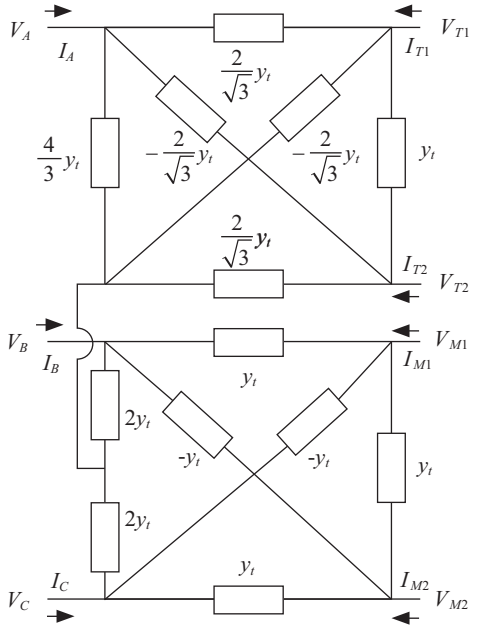

Fig. 6. Equivalent circuit of Scott connection scheme.

As shown Fig. 6, an equivalent circuit model can also be obtained using the interconnection method in which the node admittance matrix is expressed as

$$Y = \begin{bmatrix} \frac{8}{9}y_t & \frac{-4}{9}y_t & \frac{-4}{9}y_t & \frac{-4\sqrt{3}}{9}y_t & \frac{4\sqrt{3}}{9}y_t & 0 & 0 \\ \frac{-4}{9}y_t & \frac{20}{9}y_t & \frac{-16}{9}y_t & \frac{2\sqrt{3}}{9}y_t & \frac{-2\sqrt{3}}{9}y_t & -2y_t & 2y_t \\ \frac{-4}{9}y_t & \frac{-16}{9}y_t & \frac{20}{9}y_t & \frac{2\sqrt{3}}{9}y_t & \frac{-2\sqrt{3}}{9}y_t & 2y_t & -2y_t \\ \frac{-4\sqrt{3}}{9}y_t & \frac{2\sqrt{3}}{9}y_t & \frac{2\sqrt{3}}{9}y_t & \frac{2}{3}y_t & \frac{-2}{3}y_t & 0 & 0 \\ \frac{4\sqrt{3}}{9}y_t & \frac{-2\sqrt{3}}{9}y_t & \frac{-2\sqrt{3}}{9}y_t & \frac{-2}{3}y_t & \frac{2}{3}y_t & 0 & 0 \\ 0 & -2y_t & 2y_t & 0 & 0 & 2y_t & -2y_t \\ 0 & 2y_t & -2y_t & 0 & 0 & -2y_t & 2y_t \end{bmatrix} \tag{7}$$

III. CALCULATION OF SHORT CIRCUIT FAULTS

Per-unit values are used in all of the following calculations. Fig. 7 presents a power system with a three-phase to two-phase transformer. The source is a balanced three-phase 161-kV power system with Y connection operating at three voltage levels: 161-kV, 69-kV, and 27.5-kV.

Fig. 8 presents the equivalent model for the calculation of short circuits in power systems with specially connected transformers.

Let the source voltages be

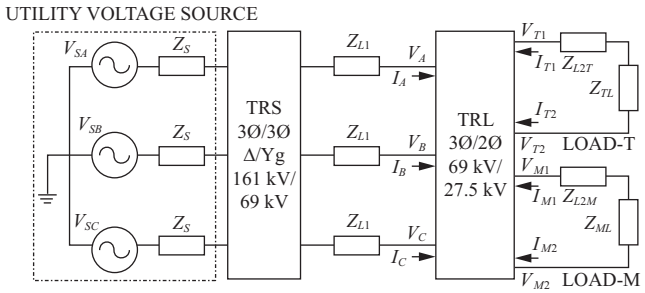

Fig. 7. Power system with specially connected transformers.

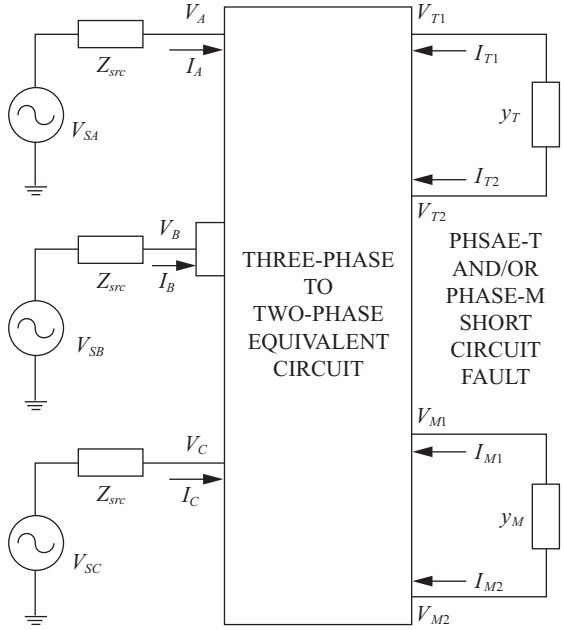

Fig. 8. Short circuit analysis of power system with specially connected transformers.

$$V_{SA} = \frac{V}{\sqrt{3}}\angle 0°,\ V_{SB} = \frac{V}{\sqrt{3}}\angle -120°,\ \text{and}\ V_{SC} = \frac{V}{\sqrt{3}}\angle 120° \tag{8}$$

The equivalent injected currents can then be expressed as follows:

$$I_{Si} = V_{Si} y_{src} \quad i = A, B, C \tag{9}$$

where $y_{src} = Z_{src}^{-1} = (Z_S + Z_{TRS} + Z_{L1})^{-1}$ and Z_{TRS} is the series impedance of the 161/69-kV transformer. The node-voltage equation for the system in this study is then given by

$$\left[I_{A,B,C,T1,T2,M1,M2} \right] = Y_e \left[V_{A,B,C,T1,T2,M1,M2} \right] \tag{10}$$

The node admittance matrix of the system in this study can be obtained using the following:

$$Y_e(m,n) = \begin{cases} Y(m,n) + y_T & m = n = 4, 5 \\ Y(m,n) - y_T & m = 4, n = 5, or, m = 5, n = 4 \\ Y(m,n) + y_M & m = n = 6, 7 \\ Y(m,n) - y_M & m = 6, n = 7, or, m = 7, n = 6 \\ Y(m,n) & others \end{cases} \tag{11}$$

where $y_T = Z_T^{-1} = (Z_{L2T} + Z_{TL} + Z_f)^{-1}$

$y_M = Z_M^{-1} = (Z_{L2M} + Z_{ML} + Z_f)^{-1}$

Z_f : fault impedance.

This indicates that

$$V_A = V_{SA} - \frac{I_A}{y_{src}},\ V_B = V_{SB} - \frac{I_B}{y_{src}},\ \text{and}\ V_C = V_{SC} - \frac{I_C}{y_{src}}$$

$$V_{T2} = V_{T1} - \frac{I_T}{y_T},\ \text{and}\ V_{M2} = V_{M1} - \frac{I_M}{y_M}$$

$$I_{T2} = -I_{T1} = I_T,\ \text{and}\ I_{M2} = -I_{M1} = I_M. \tag{12}$$

$$V_T = \frac{I_T}{y_T},\ \text{and}\ V_M = \frac{I_M}{y_M}$$

The relationship in (12) demonstrates that (10) can be re-arranged as follows:

$$f_{1,\ldots,7}(I_A, I_B, I_C, I_T, I_M, V_T, V_M) = c_{1,\ldots,7} \tag{13}$$

The iterative procedures using Newton's method are described by the following:

$$\Delta C^{(k)} = J^{(k)} \Delta X^{(k)} \tag{14}$$

$$X^{(k+1)} = X^{(k)} + \Delta X^{(k)} \tag{15}$$

where

$$\Delta X^{(k)} = \begin{bmatrix} \Delta I_A^{(k)} \\ \Delta I_B^{(k)} \\ \Delta I_C^{(k)} \\ \Delta I_T^{(k)} \\ \Delta I_M^{(k)} \\ \Delta V_T^{(k)} \\ \Delta V_M^{(k)} \end{bmatrix} \text{ and } \Delta C^{(k)} = \begin{bmatrix} c_1 - (f_1)^{(k)} \\ c_2 - (f_2)^{(k)} \\ c_3 - (f_3)^{(k)} \\ c_4 - (f_4)^{(k)} \\ c_5 - (f_5)^{(k)} \\ c_6 - (f_6)^{(k)} \\ c_7 - (f_7)^{(k)} \end{bmatrix} \tag{16}$$

The Jacobian matrix is as follows:

$$J^{(k)}=\begin{bmatrix}
(\frac{\partial f_1}{\partial I_A})^{(k)} & (\frac{\partial f_1}{\partial I_B})^{(k)} & (\frac{\partial f_1}{\partial I_C})^{(k)} & (\frac{\partial f_1}{\partial I_T})^{(k)} & (\frac{\partial f_1}{\partial I_M})^{(k)} & (\frac{\partial f_1}{\partial V_T})^{(k)} & (\frac{\partial f_1}{\partial V_M})^{(k)} \\
(\frac{\partial f_2}{\partial I_A})^{(k)} & (\frac{\partial f_2}{\partial I_B})^{(k)} & (\frac{\partial f_2}{\partial I_C})^{(k)} & (\frac{\partial f_2}{\partial I_T})^{(k)} & (\frac{\partial f_2}{\partial I_M})^{(k)} & (\frac{\partial f_2}{\partial V_T})^{(k)} & (\frac{\partial f_2}{\partial V_M})^{(k)} \\
(\frac{\partial f_3}{\partial I_A})^{(k)} & (\frac{\partial f_3}{\partial I_B})^{(k)} & (\frac{\partial f_3}{\partial I_C})^{(k)} & (\frac{\partial f_3}{\partial I_T})^{(k)} & (\frac{\partial f_3}{\partial I_M})^{(k)} & (\frac{\partial f_3}{\partial V_T})^{(k)} & (\frac{\partial f_3}{\partial V_M})^{(k)} \\
(\frac{\partial f_4}{\partial I_A})^{(k)} & (\frac{\partial f_4}{\partial I_B})^{(k)} & (\frac{\partial f_4}{\partial I_C})^{(k)} & (\frac{\partial f_4}{\partial I_T})^{(k)} & (\frac{\partial f_4}{\partial I_M})^{(k)} & (\frac{\partial f_4}{\partial V_T})^{(k)} & (\frac{\partial f_4}{\partial V_M})^{(k)} \\
(\frac{\partial f_5}{\partial I_A})^{(k)} & (\frac{\partial f_5}{\partial I_B})^{(k)} & (\frac{\partial f_5}{\partial I_C})^{(k)} & (\frac{\partial f_5}{\partial I_T})^{(k)} & (\frac{\partial f_5}{\partial I_M})^{(k)} & (\frac{\partial f_5}{\partial V_T})^{(k)} & (\frac{\partial f_5}{\partial V_M})^{(k)} \\
(\frac{\partial f_6}{\partial I_A})^{(k)} & (\frac{\partial f_6}{\partial I_B})^{(k)} & (\frac{\partial f_6}{\partial I_C})^{(k)} & (\frac{\partial f_6}{\partial I_T})^{(k)} & (\frac{\partial f_6}{\partial I_M})^{(k)} & (\frac{\partial f_6}{\partial V_T})^{(k)} & (\frac{\partial f_6}{\partial V_M})^{(k)} \\
(\frac{\partial f_7}{\partial I_A})^{(k)} & (\frac{\partial f_7}{\partial I_B})^{(k)} & (\frac{\partial f_7}{\partial I_C})^{(k)} & (\frac{\partial f_7}{\partial I_T})^{(k)} & (\frac{\partial f_7}{\partial I_M})^{(k)} & (\frac{\partial f_7}{\partial V_T})^{(k)} & (\frac{\partial f_7}{\partial V_M})^{(k)}
\end{bmatrix} \tag{17}$$

Types of system fault include the following:

(a) Two-phase balanced faults: short circuit faults in phase T as well as phase M. Short circuit faults occur under a load of 27.5-kV in phase T and phase M. Thus, $Z_{TL} = Z_{ML} = 0$, and $Z_f = 0.1$.
(b) Single-phase unbalanced faults: short circuit faults in phase T or phase M. Short circuit faults occur under a load of 27.5-kV in either phase T or phase M.
  (b1) Short circuit fault occurs in phase-T. Thus, $Z_{TL} = 0$ and $Z_f = 0.1$.
  (b2) Short circuit fault occurs in phase-M. Thus, $Z_{ML} = 0$ and $Z_f = 0.1$.

As an example, let us take a single-phase unbalanced fault in phase T on the 27.5 kV side of the power system implemented using the V-V scheme. In the initial stage, the estimation of current is

$$\begin{bmatrix} I_A^{(0)} \\ I_B^{(0)} \\ I_C^{(0)} \\ I_T^{(0)} \\ I_M^{(0)} \\ V_T^{(0)} \\ V_M^{(0)} \end{bmatrix} = \begin{bmatrix} 0 \\ 0 \\ 0 \\ 0 \\ 0 \\ 0 \\ 0 \end{bmatrix} \tag{18}$$

A solution is obtained when the absolute difference between two successive iterations is less than a specified value; i.e.,

$$\left| X^{(k+1)} - X^{(k)} \right| \le \varepsilon \tag{19}$$

where ε is the desired degree of accuracy.

Table 1. Inverse t-I curve parameter of over-current relay.

t-I curve setting		α	β
A	Normal Inverse	0.02	0.14
B	Very Inverse	1.0	13.5
C	Extremely Inverse	2.0	80.0
D	Long-Time Inverse	1.0	120.0

In stage k, when current matrix $\begin{bmatrix} I_A^{(k)} \\ I_B^{(k)} \\ I_C^{(k)} \\ I_T^{(k)} \\ I_M^{(k)} \end{bmatrix}$ is known, the bus voltage matrix $\begin{bmatrix} V_A^{(k)} \\ V_B^{(k)} \\ V_C^{(k)} \\ V_T^{(k)} \\ V_M^{(k)} \end{bmatrix}$ can be obtained using (12).

The current matrix can then be updated using (15). Eqs. (14), (16) and (17) are also used. The iteration is repeated until the error between stage k +1 and stage k is reduced to an acceptable level.

IV. EFFECTS OF OVER-CURRENT RELAY

In cases where voltage sag is caused by a fault in the power system, duration (Δt) depends on the time required to clear the fault via the operations of the protective relay and circuit breaker (CB). The relay considered in this study is an over-current relay (50/51). The operating time of the relay can be derived from the movement curve. The operating time of the circuit breaker is related to the mechanical characteristics of the device, and is therefore regarded as a constant value. The duration of voltage sag can be expressed as follows:

$$\Delta t = t_{Ry} + t_{CB} \tag{20}$$

where t_{Ry} is the operating time of the protective relay and t_{CB} is the operating time of the circuit breaker.

In practical distribution systems, t_{CB} is generally between 3 and 8 cycles (IEEE Standard, Vol. 1100, 2005).

According to the IEC 60255-22 Standard (Hung et al., 2012), the inverse t-I curve parameters of the over-current relay (51) are presented in (21). The α and β values in Table 1 are used to determine the slopes.

$$t_{Ry}(s) = \frac{k\beta}{\left(\frac{I_F}{I_P}\right)^{\alpha} - 1} \tag{21}$$

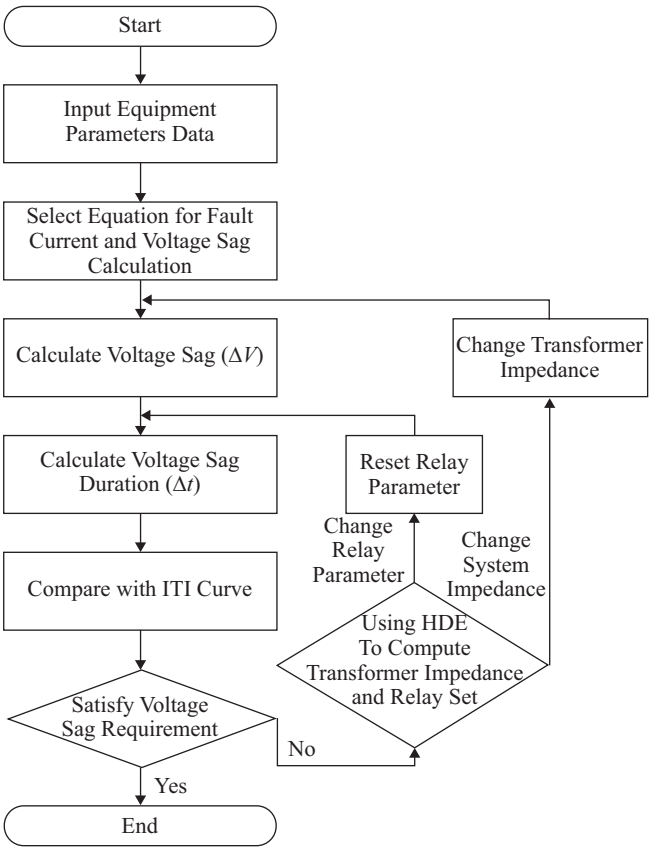

Fig. 9. Flowchart showing calculation of voltage sag.

where k is the time multiplier,
I_F is the fault current detected by relay (normally the effective value), and
I_P is the current setting threshold.

If the normal inverse curve is used, then $\alpha = 0.02$ and $\beta = 0.14$ can be substituted into (21) to obtain the duration of voltage sag. The value of $\Delta V_{(F)} \times \Delta t_{(F)}$ can be used to describe the range of voltage sag in which $\Delta V_{(F)}$ is the drop in voltage and $\Delta t_{(F)}$ is the duration. Fig. 10 shows that

$$\Delta V_{(F)} = V_{SFi} - \frac{I_{Fi}}{y_{src}} \tag{22}$$

where $i = A$, B, and C. If $I_{Fi} \geq I_p$, then

$$\Delta t_{(F)} = \frac{0.14k}{\left|\frac{I_{Fi}}{I_P}\right|^{0.02} - 1} \tag{23}$$

V. VOLTAGE SAG ANALYSIS

Fig. 9 presents a flowchart illustrating the process of calculating voltage sag, which is as follows:

(1) Transformation of impedances of system equipment into pu values and data related to the input parameters.
(2) Selection of equation used for the calculation of fault voltages and currents at all voltage levels to obtain the range of voltage sag $\Delta V_{(F)}$.
(3) Selection of curve related to the over-current relay (50/51). The operating times of the relay and circuit breaker are added to obtain the fault clearing time, which represents the duration of voltage sag $\Delta t_{(F)}$.
(4) Comparison of $\Delta V_{(F)}$ and $\Delta t_{(F)}$ with the ITI curve to determine whether the voltage sag satisfies the requirements of the ITI curve.
(5) In cases where the calculated voltage sag and duration are not acceptable, HDE is used to compute the appropriate impedance of the transformer and parameter settings for the relay.
(6) The process is repeated iteratively until voltage sag and duration have been reduced to an acceptable level through the adjustment of transformer impedance and relay parameters.

VI. PROBLEM FORMULATION

The HDE method is used to obtain suitable values for transformer impedance and relay settings, as follows:

1. Objective Function

$$\text{Minimize } M = \sqrt{(t_{ITIc} - t_{up})^2 + \rho(V_{ITIc} - V_{up})^2} \tag{24}$$

where t_{ITIc}: ITI curve duration
V_{ITIc}: ITI curve voltage
t_{up}: fault duration time of unacceptable point
V_{vp}: fault voltage of unacceptable point
where $\rho = 1$
and $t_{ITIc} \leq t_{up} \bigcap V_{ITIc} \geq V_{up}$, otherwise $M = 0$,
and variable vector: $X = \begin{bmatrix} X_{TRS} & X_{TRL} & k \end{bmatrix}^t$

$$k^{\min} < k < k^{\max}$$

$$X_{TRq}^{\min} < X_{TRq} < X_{TRq}^{\max} \quad q = S, L \tag{25}$$

where k: relay time multiplier, and
X_{TRS} and X_{TRL}: transformer impedance.

2. Constraints

(a) Limitations regarding system equipment must be taken into account.
(b) Voltage regulation must be below 5%; i.e.,

$$-5\% < VR_i < 5\% \quad i = A, B, C \tag{26}$$

(c) The duration of actions taken by the downstream relay must be less than that of the upstream relay; i.e.,

Table 2. System data.

Power Source	Balanced three-phase, 161 kV, Y-connected, X/R = 33.25, short circuit capacity = 10935 MVA
Transformer	TRS: 3Φ/3Φ, 161/69 kV, 200 MVA, X_{TRS} = 13%, X/R = 40, Δ/Y-g connected, Z_{g1} = 20 Ω
	TRL: 3Φ/2Φ, 69/27.5 kV, 30 MVA, X_{TRL} = 10%, X/R = 10
Line	Z_{L1} = 1.1869 + j3.9108 Ω
	$Z_{L2T} = Z_{L2M}$ = 0.873 + j2.295 Ω
Load	Each of phase T and phase M: 5MW + j3MVAR
Circuit breaker	t_{CB} = 0.08 s

Table 3. Original settings used to determine inverse t-I curve of protective relay.

Voltage level	Time multiple (k)
27.5 kV	0.1
69 kV	0.2

Table 4. Calculation results for 69-kV bus associated with a two-phase balanced fault on the 27.5-kV load bus of system operating under original parameter settings (t_{CB} = 0.08 s).

specially connected transformers	Phase	Fault voltage (pu)	Fault current (pu)	Fault clearing time Δt (s)
V-V	Phase-A	0.7759	8.50	0.3455
	Phase-B	0.5924	13.06	
	Phase-C	0.7533	8.16	
Scott	Phase-A	0.6848	10.13	0.3682
	Phase-B	0.6677	10.72	
	Phase-C	0.6677	10.61	

$$T_{F,27.5kV} < T_{F,69kV} \tag{27}$$

VII. SIMULATION RESULTS

In the following, we consider two-phase balanced faults and single-phase unbalanced faults. Fig. 7 presents the simulation system, the parameters of which are listed in Table 2. The relay follows the normal inverse curve, where α is 0.02 and β is 0.14. Table 3 lists the original settings.

1. Two-Phase Balanced Fault

Table 4 presents the calculation of 69-kV bus voltages when a two-phase balanced fault occurs on the 27.5-kV load bus in a system operating under the original settings. Fig. 10 presents a comparison of voltage sag values *vs.* ITI curves, in which the voltage sag values at the 69-kV bus are below the curve when using the original settings.

The HDE approach is used to determine suitable values for the transformer impedance and relay k. Table 5 lists the original settings and limitation conditions. Table 6 lists the parameter values obtained using the HDE method. Table 7 lists the calculation results for a 69-kV bus within a system operating under parameter values obtained using the HDE method. Fig. 10 presents a comparison of these values with

Table 5. Original settings and limitation conditions.

System parameter		Original setting	Limitation
transformer	TRS 3Φ/3Φ 161/69 kV 200 MVA	X_{TRS} = 13%	7% ≦ X_{TRS} ≦ 13%
	TRL 3Φ/2Φ 69/27.5 kV 30 MVA	X_{TRL} = 10%	10% ≦ X_{TRL} ≦ 16%
relay	CO-k	k = 0.1	0.01 ≦ k ≦ 0.1

Table 6. Parameter values obtained using HDE.

	X_{TRS}	X_{TRL}	k
V-V	7%	16%	0.01
Scott	7%	15.2%	0.01

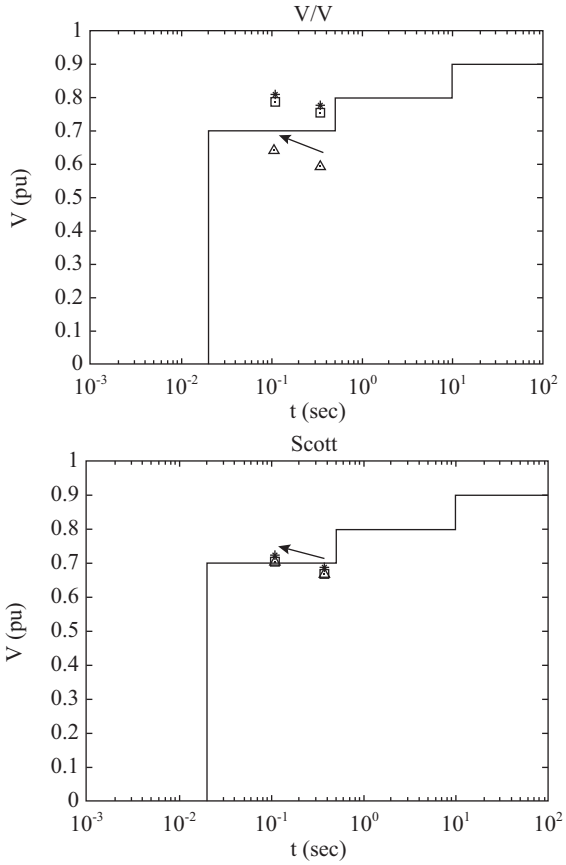

Fig. 10. Comparison of voltage sag values with ITI curve for 69-kV bus on system with a two-phase balanced fault on 27.5 kV load bus operating under the original parameter settings and those obtained using HDE (star: V_A, triangle: V_B, square: V_C).

Table 7. Calculation results of 69-kV bus associated with a two-phase balanced fault on the 27.5-kV load bus of system operating under parameter values obtained using HDE (t_{CB} = 0.08s).

Specially connected transformers	Phase	Fault voltage (pu)	Fault current (pu)	Fault clearing time Δt (s)
V-V	Phase-A	0.8085	7.75	0.10737
	Phase-B	0.6401	12.11	
	Phase-C	0.7849	7.46	
Scott	Phase-A	0.7222	9.37	0.10950
	Phase-B	0.7009	10.16	
	Phase-C	0.7001	10.03	

Table 8. Calculation results for 69-kV bus for a single-phase unbalanced fault (phase T) on the 27.5 kV load bus of a system operating under the original parameter settings (t_{CB} = 0.08 s).

Specially connected transformers	Phase	Fault voltage (pu)	Fault current (pu)	Fault clearing time Δt (s)
V-V	Phase-A	0.7972	8.74	0.3959
	Phase-B	0.7511	8.68	
	Phase-C	0.9910	0.30	
Scott	Phase-A	0.6845	10.13	0.3754
	Phase-B	0.9082	4.88	
	Phase-C	0.9406	5.26	

Table 9. Calculation results for 69-kV bus for a single-phase unbalanced fault (phase T) on the 27.5 kV load bus of system operating under parameter values determined using HDE (t_{CB} = 0.08s).

specially connected transformers	Phase	Fault voltage (pu)	Fault current (pu)	Fault clearing time Δt (s)
V-V	Phase-A	0.8244	7.96	0.11305
	Phase-B	0.7804	7.91	
	Phase-C	0.9913	0.30	
Scott	Phase-A	0.7222	9.37	0.11059
	Phase-B	0.9162	4.51	
	Phase-C	0.9474	4.88	

ITI curves. When the transformer impedance values and relay settings were modified using the HDE method, the voltage values increased and the duration values decreased.

2. Single-Phase Unbalanced Fault

As shown in Fig. 8, a short circuit fault occurred on the 27.5-kV load bus in phase T. Table 8 lists the results for the 69-kV bus on a system using the original settings. Fig. 11 compares voltage sag values on the 69-kV bus with the ITI curve. Table 9 presents the simulation results for the 69-kV bus on a system with parameter values determined using HDE. Fig. 11 also compares the 69-kV bus voltage values with the

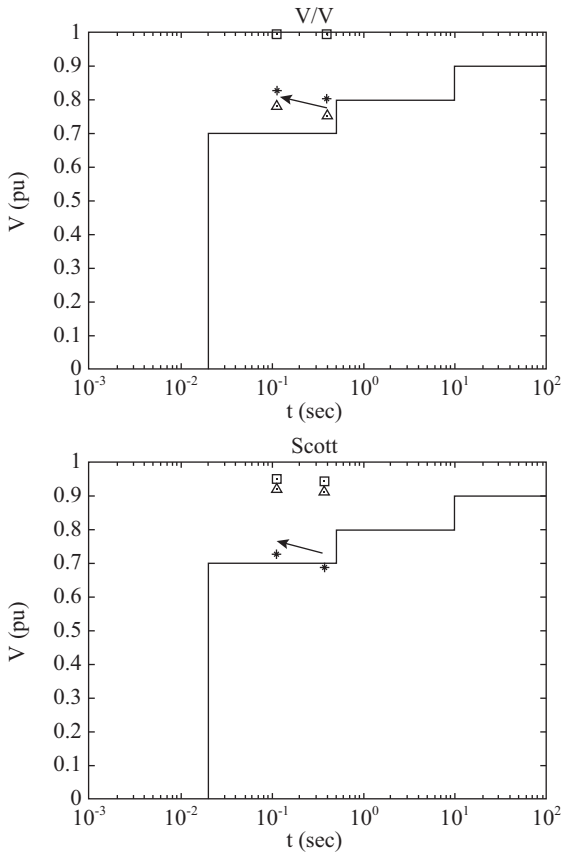

Fig. 11. Comparison of voltage sag values on 69-kV bus with ITI curve of system with a single-phase unbalanced fault (phase T) on the 27.5kV load bus with original parameter values and those determined using HDE (star: V_A, triangle: V_B, square: V_C).

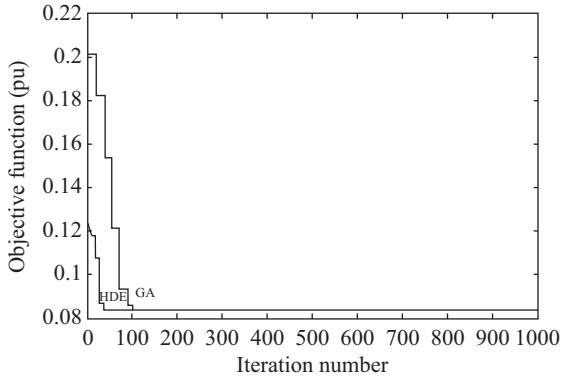

Fig. 12. Comparison of HDE and GA with regard to convergence characteristics related to two-phase fault on system using Scott scheme.

ITI curve, in which the severity of the voltage sag was reduced.

To evaluate the effectiveness of the proposed method, we conducted a comparison of HDE and a genetic algorithm (GA) for a two-phase fault in a system using the Le Blanc scheme, as shown in Fig. 12. HDE required 38 iterations, whereas the

Table 10. Comparison of HDE and GA with regard to a two-phase fault occurring on system with Scott scheme.

HDE		GA	
Objective function (p.u.)	0.0001	Objective function (p.u.)	0.0001
N_P	5	N_P	70
C_R	0.5	Pc	0.8
Iteration number	38	Iteration number	128
F	0.01	Pm	0.05
$\varepsilon 1$	0.1		
$\varepsilon 2$	0.1		

Table 11. Probability distributions of circuit breaker operation and fault type.

	Type	Probability
Circuit breaker	success	0.95
	fail	0.05
Fault type	two-phase balanced fault	0.20
	single-phase unbalanced fault (T)	0.40
	single-phase unbalanced fault (M)	0.40

Table 12. Design results.

Specially connected transformers	Phase	Original objective function (p.u.)			HDE method objective function (p.u.)			
		two-phase balanced fault	single-phase unbalanced fault (T)	single-phase unbalanced fault (M)	two-phase balanced fault	single-phase unbalanced fault (T)	single-phase unbalanced fault (M)	Expected value (p.u.)
V-V	Phase-A	0.0001	0.0001	0.0001	0.0001	0.0001	0.0001	0.0025
	Phase-B	0.1076	0.0001	0.0001	0.0599	0.0001	0.0001	0.0181
	Phase-C	0.0001	0.0001	0.0001	0.0001	0.0001	0.00001	0.0036
Scott	Phase-A	0.0152	0.0155	0.0001	0.0001	0.0001	0.0001	0.0054
	Phase-B	0.0323	0.0001	0.0001	0.0001	0.0001	0.0001	0.0042
	Phase-C	0.0323	0.0001	0.0001	0.0001	0.0001	0.0001	0.0048

GA required 128 generations to achieve convergence. As shown in Table 10, HDE is clearly faster than the GA and the results for the objective function are lower.

VIII. CIRCUIT BREAKER AND FAULT TYPE UNCERTAINTY

In previous sections, voltage sags are determined under set parameters. However, since in practice circuit breakers and fault types vary, so do operating conditions. Despite the care taken in determining the transformer impedance and relay settings, problems of reliability persist due to process variation in manufacturing as well as the aging of devices after installation. Expectation and standard deviation concepts can be used. Table 11 presents the probability distributions of circuit breaker operation and fault types. Table 12 also gives the planning results considering expectation. The proposed method also gives the lowest expectation of the objective function.

IX. CONCLUSIONS

This study developed models of specially connected transformers for use in fault analysis with a focus on V-V and Scott connection schemes. The severity of voltage sag in a system with specially connected transformers can be controlled by adjusting the impedance of transformers and relay settings. The node admittance matrix of each scheme was obtained to facilitate the calculation of voltage sag. We also developed an optimization approach using the HDE method to identify suitable values for transformer impedance and relay settings. Our results were the compared with ITI curves. Simulation results demonstrate the efficacy of the proposed method in reducing voltage sag, and the Scott better than V-V connection. The uncertain condition is also considered by using the probability concept.

REFERENCES

Bollen, M. H. J. (1999). Understanding Power Quality Problems: Voltage Sags and Interruptions. IEEE Press Series on Power Engineering, New York, USA.

Chang, Y. P. and C. J. Wu (2005). Optimal multi-objective planning of large-scale passive harmonic filters using hybrid differential evolution method considering parameter and loading uncertainty. IEEE Transactions on Power Delivery 20, 408-416.

Chen, T. H. (1994). Simplified models of electric substations for three-phase power-flow studies. Proceeding of the 29th IAS Annual Meeting, Denver, Colorado, USA, 3, 2245-2248.

Chen, T. H. and H. Y. Kuo (1995). Network modeling of traction substation transformers for studying unbalance effects. IEE Proceedings- Generation Transmission and Distribution 142(2), 103-108.

Chiou, J. P. and F. S. Wang (1998). A hybrid method of differential evolution with application to optimal control problems of a bioprocess system. Proceedings of the IEEE International Conference on Evolutionary Computation, 627-632.

Das, J. C. (1990). Effects of momentary voltage dips on the operation of induction and synchronous motors. IEEE Transactions on Industry Applications 26, 711-718.

Gomez, J. C. and M. M. Morcos (2002a). Coordinating overcurrent protection and voltage sag in distributed generation system. IEEE Power Engineering Review 22, 16-19.

Gomez, J. C. and M. M. Morcos (2002b). Voltage sag and recovery time in repetitive events. IEEE Transactions on Power Delivery 17, 1037-1043.

Heydt, G. T. and W. T. Jewell (1998). Pitfalls of electric power quality indices. IEEE Transaction on Power Delivery 13, 570-578.

Heydt, G. T., R. Ayyanar and R. Thallam (2001). Power Acceptability. IEEE Power Engineering Review 21, 12-15.

Huang, C. P., C. J. Wu, Y. S. Chuang, S. K. Peng, J. L. Yen and M. H. Han (2006). Loading characteristics analysis of specially connected transformers using various power factor definitions. IEEE Transaction on Power Delivery 21, 1406-1413.

Huang, S. R., Y. L Kuo., B. N. Chan, K. C. Lu and M. C. Huang (2001). A short circuit current study for the power supply system of Taiwan railway. IEEE Transactions on Power Delivery 16, 492-497.

Hung, C. M., S. J. Chen, Y. C. Huang and H. T. Yang (2012). Comparative study of evolutionary computation methods for active-reactive power dispatch. IET Generation, Transmission and Distribution 6, 636-645.

IEEE Recommended Practice for Emergency and Standby Power Systems for Industrial and commercial Applications. IEEE Standard, 446 (1995).

IEEE Recommended Practice for Monitoring Electric Power Quality. IEEE Standard, 1159 (1995).

IEEE Recommended Practice for Powering and Grounding Electronic Equipment. IEEE Standard, 1100 (2005).

Kyei, J., R. Ayanar, G. Heydt and R. Thallam (2002). The design of power acceptability curves. IEEE Transactions on Power Delivery 17, 828-833.

Lee, G. J., M. M. Albu and G. T. Heydt (2004). A power quality index based on equipment sensitivity, Cost, and Network Vulnerability. IEEE Transactions on Power Delivery 19, 1504-1510.

Lin, Y. C., K. S. Hwang and F. S. Wang (2000). Plant scheduling and planning using mixed-integer hybrid differential evolution with multiplier updating. Proceedings of the IEEE Congress on Evolutionary Computation 1, 593-600.

Mahdianpoor, F. M., R. A. Hooshmand and M. Ataei (2011). A new approach to multifunctional dynamic voltage restorer implementation for emergency control in distribution systems. IEEE Transactions on Power Delivery 26, 882-890.

Wang, J., S. Chen and T. T. Lie (2005). System voltage sag performance estimation. IEEE Transactions on Power Delivery 20, 1738-1747.

Yalcinkaya, G., M. H. J. Bollen and P. A. Crossley (1998). Characterization of voltage sags in industrial distribution systems. IEEE Transactions on Industry Applications 34, 682-688.